Journal of Power Sources 196 (2011) 2264–2268

Contents lists available at ScienceDirect

Journal of Power Sources

journal homepage: www.elsevier.com/locate/jpowsour

Short communication

Limiting current density in bis(trifluoromethylsulfonyl)amide-based ionic liquid for lithium batteries

Jun-Woo Park, Kazuki Yoshida, Naoki Tachikawa, Kaoru Dokko, Masayoshi Watanabe*

Department of Chemistry and Biotechnology, Yokohama National University, 79-5 Tokiwadai, Hodogaya-ku, Yokohama 240-8501, Japan

ARTICLE INFO

Article history:
Received 31 July 2010
Received in revised form
20 September 2010
Accepted 22 September 2010
Available online 1 October 2010

Keywords:
Lithium batteries
Ionic liquid
Mass transport
Limiting current density

ABSTRACT

The physicochemical and electrochemical properties of the binary ionic liquid (IL), lithium bis(trifluoromethylsulfonyl)amide (LiTFSA) dissolved in *N*,*N*-diethyl-*N*-methyl-*N*-(2-methoxyethyl)ammonium bis(trifluoromethylsulfonyl)amide (DEMETFSA), were investigated. The ionic conductivity of the binary IL decreased with an increase in LiTFSA concentration. The self-diffusion coefficients of Li^+, $DEME^+$, and $TFSA^-$ dissolved in the IL were measured by using the pulsed-field-gradient spin-echo (PGSE) NMR method. The self-diffusion coefficient of each ionic species was also found to decrease with increasing concentration of LiTFSA. The limiting current density in the IL electrolyte was evaluated by chronoamperometry using symmetric Li|IL|Li cell. The results suggest that the diffusion process of Li(I) in the IL dominates the limiting current density in the cell. The highest limiting current density is achieved at a concentration of 0.64 mol dm^{-3} of LiTFSA.

1. Introduction

Ionic liquids (ILs) have recently attracted considerable attention, and they are expected to have a wide range of applications. ILs combine unique properties such as wide liquid temperature range and negligible vapor pressure with high thermal and electrochemical stability. To date, electrochemists have attempted to use ILs as new electrolytes in electrochemical devices. For example, ILs are among the most attractive nonflammable electrolytes that can be used for achieving high thermal stability in lithium ion batteries. There have been many reports on the use of bis(trifluoromethylsulfonyl)amide ($TFSA^-$)-based ILs as possible electrolytes for lithium ion batteries [1–17]. In these studies, the high thermal stability of $TFSA^-$-based ILs, even when they are in contact with charged electrode materials, was demonstrated [11,17]; stable charge–discharge operations using either half cells or full cells were also demonstrated [1–16]. In light of these findings, the charge–discharge rate capabilities of Li|IL|$LiCoO_2$ cells were evaluated by different research groups [4,5,10]. However, typical ILs are approximately two orders of magnitude higher in viscosity than conventional organic electrolytes. It was therefore anticipated that electrolytes having such high viscosity would limit the mobility of the Li(I) species and consequently the charge–discharge capability of the lithium batteries. In the past, the diffusion coefficient of Li(I) has been estimated by means of cyclic voltammetry [18] and pulsed-field-gradient spin-echo (PGSE) NMR [19–23] and it was found to be approximately equal to 10^{-8}–10^{-7} cm^2 s^{-1}. However, the maximum current density in a battery with IL electrolytes has not been thus far thoroughly investigated. In a lithium ion battery, the cathode and anode are separated by a porous film with a thickness of ca. 20–30 μm; therefore, the Li(I) transport between cathode and anode takes place in a finite space. It is important to perform a quantitative study of the relationship between the Li(I) transport properties in an IL and the limiting current density in a finite space.

In this study, the binary IL, lithium bis(trifluoromethylsulfonyl)amide (LiTFSA) dissolved in *N*,*N*-diethyl-*N*-methyl-*N*-(2-methoxyethyl)ammonium bis(trifluoromethylsulfonyl)amide (DEMETFSA), was chosen as a model IL. This choice was based on past experiments of Seki et al. [13,14] who verified the stable charge–discharge operation of Li|LiTFSA/DEMETFSA binary IL|$LiCoO_2$. In this study, we investigated physicochemical properties such as ionic conductivity, viscosity, and self-diffusion coefficients of the LiTFSA/DEMETFSA binary IL. Furthermore, the limiting current density in this IL was evaluated through a series of very simple experiments using a symmetric Li|IL|Li cell.

2. Experimental

DEMETFSA was purchased from Kanto Kagaku and used as received. LiTFSA (3M Company) was dissolved into DEMETFSA in order to prepare the binary IL electrolyte. The viscosity of the final IL was measured using a cone-plate viscometer (Physica MCR, Anton Paar). Density measurements were performed using a thermoregulated density/specific gravity meter DA-100 (Kyoto Electronics

* Corresponding author. Tel.: +81 45 339 3955; fax: +81 45 339 3955.
E-mail address: mwatanab@ynu.ac.jp (M. Watanabe).

0378-7753/$ – see front matter © 2010 Elsevier B.V. All rights reserved.
doi:10.1016/j.jpowsour.2010.09.067

Table 1
The molar ratio of Li^+, $DEME^+$, and $TFSA^-$, along with the density, and $\sigma_{Imp}/\sigma_{NMR}$ value for the different LiTFSA/DEMETFSA binary ILs at 30 °C.

LiTFSA concentration (mol dm^{-3})	Molar ratio			Density (g cm^{-3})	$\sigma_{Imp}/\sigma_{NMR}$
	Li^+	$DEME^+$	$TFSA^-$		
0.00	0.00	0.50	0.50	1.41	0.67
0.14	0.02	0.48	0.50	1.42	0.62
0.42	0.06	0.44	0.50	1.44	0.57
0.64	0.09	0.41	0.50	1.46	0.52
0.86	0.11	0.39	0.50	1.47	0.50
1.16	0.15	0.35	0.50	1.50	0.50

Manufacturing). The ionic conductivity of the IL under study was estimated through complex impedance measurements, performed with the use of a computer-controlled impedance analyzer (VMP2, Princeton Applied Research). For this purpose, the IL was poured into an airtight cell consisting of two platinum electrodes, and then, the impedance measurements were performed at 30 °C. The self-diffusion coefficients for Li^+, $DEME^+$, and $TFSA^-$ were measured by PGSE-NMR (JNM-AL 400, JEOL). Details of the PGSE-NMR measurements have been reported elsewhere [24–26].

A symmetric cell, Li|LiTFSA/DEMETFSA binary IL|Li, was fabricated to study the electrochemical properties of the LiTFSA/DEMETFSA electrolyte. More specifically, the symmetric configuration was implemented in a way that the final cell resembles the common CR 2032 type cell. Two Li metal foils were cut into disk shape (16 mm in diameter) and used as electrodes. A porous polyethylene sheet (Celgard® 2730, 21 μm-thick and with 43% porosity) was added to separate the two Li electrodes. In other words, the electrolyte was kept within voids of the porous separator. All materials were handled in an argon-filled glove box (VAC, dew point <−80 °C). Electrochemical measurements were conducted using the computer-controlled potentio/galvanostat, VMP2. After the cell fabrication was completed, a voltage of 10 mV was applied for 1200 s to the newly developed cell in order to obtain a fresh lithium metal surface by stripping and deposition of Li at the anode and cathode, respectively. Subsequently, the cell was kept in an open circuit for two days. The AC impedance measurements were performed at open circuit voltage with a peak-to-peak amplitude of 10 mV and frequency ranging from 500 kHz to 20 mHz. The open circuit potential was confirmed to be lower than 1 mV before we started the impedance measurements. More specifically, DC polarization was conducted at different controlled voltage stepped from open circuit voltage (OCV < 3 mV). All the electrochemical measurements were carried out at 30 °C.

3. Results and discussion

The density of the LiTFSA/DEMETFSA binary IL was found to increase with increasing LiTFSA concentration (C_{Li}), as shown in Table 1. Fig. 1(a) shows the viscosity (η) and ionic conductivity (σ_{Imp}) as a function of C_{Li}. We noted that the ionic conductivity decreases with increasing C_{Li}, a decrease which was mainly due to an increase in viscosity, a phenomenon that has been widely reported [2,3,10,15,27]. The high viscosity of the LiTFSA/DEMETFSA system resulted in a lower ionic conductivity than typical organic electrolytes [28]. The self-diffusion coefficients of Li^+, $DEME^+$, and $TFSA^-$ measured by means of PGSE-NMR are shown in Fig. 1 (b). The diffusion coefficient for each ionic species ranges from 10^{-8} to 10^{-7} cm^2 s^{-1}. The self-diffusion coefficients were also found to decrease with increasing C_{Li}. The ionic conductivity (σ_{NMR}) was calculated based on the experimentally estimated self-diffusion coefficient with the use of the Nernst–Einstein Eq. (1) and the assumption that salts are completely dissociated in the liquid [29]:

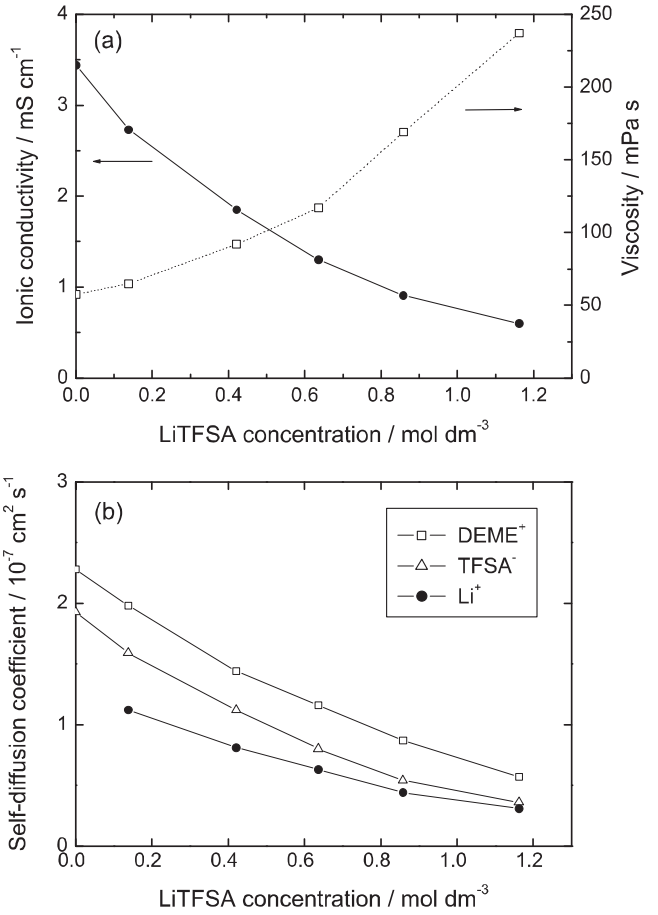

Fig. 1. (a) Viscosity and ionic conductivity of LiTFSA/DEMETFSA binary ILs. (b) Self-diffusion coefficients for the $DEME^+$, Li^+, $TFSA^-$ in ILs as a function of the LiTFSA concentration at 30 °C.

$$\sigma_{NMR} = \frac{e^2}{kT}(N_{Li^+}D_{Li^+} + N_{DEME^+}D_{DEME^+} + N_{TFSA^-}D_{TFSA^-}) \quad (1)$$

where e is the electric charge on each ionic carrier, k is the Boltzmann constant, T is the absolute temperature, N_X ($X = Li^+$, $DEME^+$, and $TFSA^-$) is the number of X ions in a unit volume, and D_X is the self-diffusion coefficient of X which is determined by the PGSE-NMR method. The ionic conductivity estimated based on the diffusivity (σ_{NMR}) was higher than σ_{Imp}, a difference that can be attributed to the interaction between ionic species and the formation of ion pairs and aggregates. Nonetheless, such the ionic aggregation is a phenomenon that evolved both in time and space and such aggregations were not considered to be static. The $\sigma_{Imp}/\sigma_{NMR}$ ratio was defined as the ionicity, or in other words, the dissociativity of the IL [24–26,29]. The value of the $\sigma_{Imp}/\sigma_{NMR}$ ratio was found to decrease with increasing C_{Li} (Table 1). By dissolving Li salts into DEMETFSA, the coordination of Li^+ cations with two $TFSA^-$ anions and the formation of Li(I) oligomeric species have been reported to occur because of the strong Lewis acidity of Li^+ cations [30]. The formation of such complex structures in the IL brought about an increase in the viscosity of IL. These strong interactions between Li^+ cations and $TFSA^-$ anions in the IL may further cause a decrease in the $\sigma_{Imp}/\sigma_{NMR}$ ratio as C_{Li} is increased. This hypothesis was supported by the fact that the difference between the values of D_{Li^+} and D_{TFSA^-} became less pronounced with increasing C_{Li} (Fig. 1(b)), though the diffusion coefficients of $TFSA^-$ bound to Li^+ and free $TFSA^-$ could not be distinguished by PGSE-NMR.

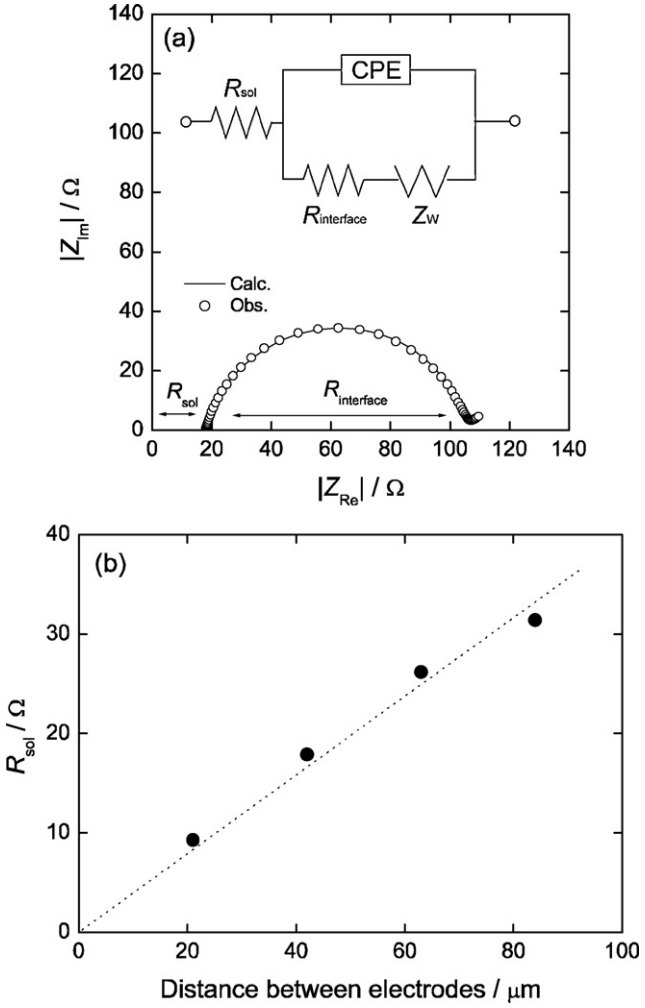

Fig. 2. (a) Nyquist plots for a symmetric Li|IL with separator|Li cell. The LiTFSA concentration C_{Li} was equal to 0.64 mol dm^{-3}, and the distance between two Li electrodes (l) was 42 μm. The inset is the schematic diagram of the equivalent circuit model used to simulate the impedance spectra and (b) solution resistance, R_{sol}, as a function of distance between two Li electrodes.

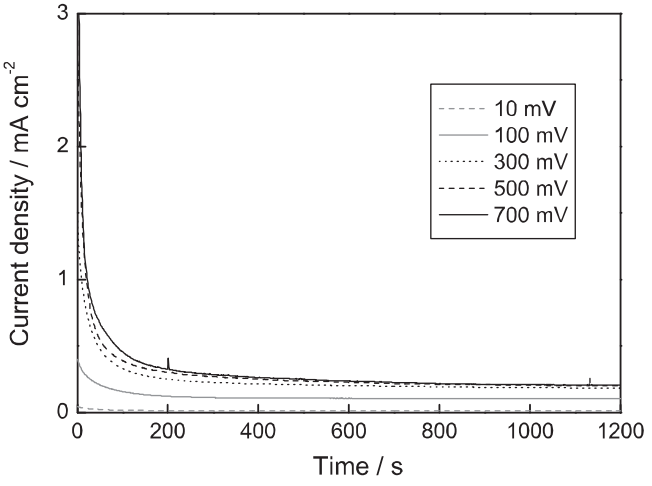

Fig. 3. Chronoamperograms for a symmetric Li|IL with separator (C_{Li} = 0.64 mol dm^{-3}, l = 42 μm)|Li cell measured at various cell voltages.

To investigate in more detail the mass transport phenomena taking place in the electrolyte during electrochemical reactions, a symmetric Li|IL|Li cell was assembled. Fig. 2(a) shows the Nyquist plots for a symmetric Li|0.64 mol dm^{-3} LiTFSA/DEMETFSA with dual separators|Li cell. These Nyquist plots were produced by means of a modified Randles-type equivalent circuit, in which the double-layer capacitor had been replaced with a constant phase element (CPE). The solution resistance (R_{sol}) was estimated to be equal to 18 Ω, and the interfacial resistance of the Li metal electrode|electrolyte ($R_{interface}$) 88 Ω. The distance between two Li electrodes changed with varying the number of separator sheets. Fig. 2(b) shows the dependence of R_{sol} on the distance between the two Li electrodes. Because R_{sol} changes linearly with the distance between the two electrodes, it can be approximated with the following expression [31,32]:

$$R_{sol} = \frac{l\tau}{A\varepsilon\sigma_{Imp}} \quad (2)$$

where l is the distance between two Li electrodes, A is the area of each electrode (2 cm^2), ε is the porosity and τ is the tortuosity factor of the separator, and lastly, σ_{Imp} is the ionic conductivity of the electrolyte. From the dependence of R_{sol} on l, the tortuosity factor was estimated to be 4.4. This value implies that the pathway for the mass transport in the separator is 4.4 times longer than the thickness of separator.

Fig. 3 shows chronoamperograms for a Li|0.64 mol dm^{-3} LiTFSA in DEMETFSA with dual separators|Li cell measured under different polarization voltages. Large currents were observed after polarization. However, as the currents decayed gradually, steady-state currents were observed. The large current after the polarization is attributed to the formation of a concentration gradient of Li(I) in the electrolyte between the cathode and the anode. The current decays because the Li(I) transference number is less than unity. The polarized $DEME^+$ and $TFSA^-$ cannot be discharged at the electrodes; this causes the concentration polarization of LiTFSA to propagate throughout the electrolyte. The steady-state current corresponds to the current carried entirely by Li(I). We regarded the current measured at 1200 s as the steady-state current (I_∞) because the decrease in the current during the interval from 1100 s to 1200 s is less than 2%. Fig. 4(a) shows the steady-state current densities estimated based on chronoamperometry measurements (Fig. 3) as a function of the applied voltage. The steady-state current density increases as the applied voltage increases in the range from 0 to 0.2 V, suggesting that the steady-state current is not controlled by diffusion processes but by the charge migration and charge transfer process at the Li|IL interface. On the other hand, the steady-state current density was independent of the applied voltage, when the latter is in the range of 0.2–1.0 V. This finding suggests that the limiting current should be attributed to the diffusion-limited process of electrochemically reactive species of Li(I). The diffusion of Li(I) occurs in the finite space between two Li electrodes. In this case, therefore, the thickness of the diffusion layer corresponds to the thickness of the separator. Furthermore, it can be controlled by varying the number of separator sheets. To confirm this, the dependence of limiting current density on the distance (l) between two Li electrodes was evaluated using the chronoamperometry measurements. Fig. 4(b) shows the limiting current density as a function of the reciprocal of l. The distance l is controlled by changing the number of separator sheets. We found that the limiting current density decreases with increasing number of separator sheets. This was attributed to the dependence of the limiting current on the Li(I) diffusion-controlled current under the finite conditions; that is, the Li(I) concentration gradient becomes smaller as the distance between the two electrodes is increasing. However, the limiting current density deviates from the linear relation at relatively larger l (smaller $1/l$) probably due to the presence of convection in the electrolyte.

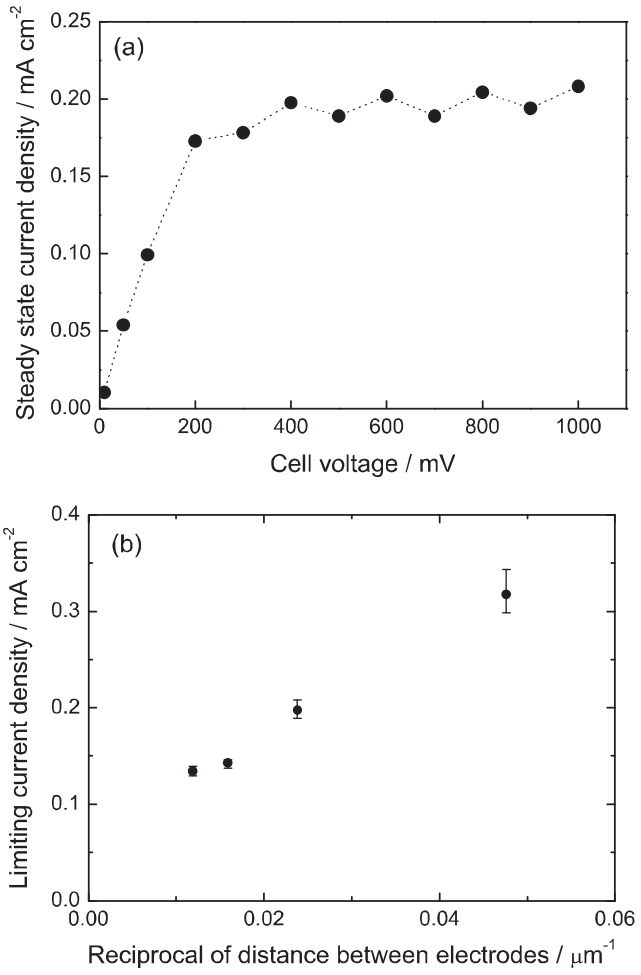

Fig. 4. (a) Steady-state current density observed for the symmetric Li|IL with separator (C_{Li} = 0.64 mol dm^{-3}, l = 42 μm)|Li cell at various cell voltages. (b) Limiting current density for Li|IL with separator (C_{Li} = 0.64 mol dm^{-3})|Li coin cell as a function of distance between two Li electrodes (l).

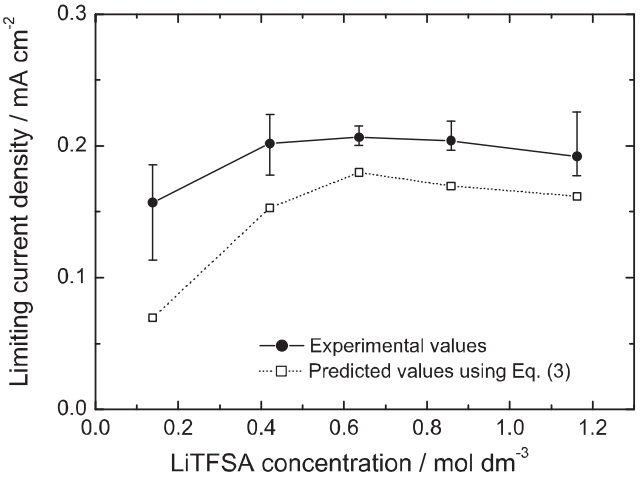

Fig. 5. Limiting current density for the symmetric Li|IL with separator (l = 42 μm)|Li cell as a function of the LiTFSA concentration. The circle and square symbols represent the limiting current density measured by chronoamperometry and the values predicted using Eq. (3) and self-diffusion coefficient of Li(I), respectively.

Fig. 5 shows the limiting current density as a function of C_{Li}. It should be noted that the limiting current density demonstrates a convex curvature, with a maximum at 0.64 mol dm^{-3}. This result does not agree with the ionic conductivity which simply decreases with an increase in LiTFSA concentrations, as shown in Fig. 1(a). As for the total ionic conductivity (Fig. 1), the total number of charge carriers (DEME$^+$, Li$^+$, TFSA$^-$) does not change considerably since the changes observed in the ionicity (dissociativity) and density after the addition of LiTFSA are relatively small (Table 1). Thus, the viscosity increase (Fig. 1) simply depresses the mobility of the charge carriers, resulting in a decrease in the ionic conductivity. On the other hand, the limiting current is determined by the Li(I) diffusion flux, and thus, where its maximum would be observed is due to the inverse effect of the LiTFSA concentration on the number of Li(I) species and the diffusivity. LiTFSA/DEMETFSA binary IL has an optimum LiTFSA concentration at 0.64 mol dm^{-3} with respect to enhancement of the Faradaic current under Li(I) diffusion-limited conditions or, in other words, under highly polarized conditions. It was made clear that the limiting current is the result of a delicate balance between the diffusivity and the number of electrochemically reactive species, namely, the Li(I) diffusion flux.

The limiting current density (I_{lim}) can be approximately predicted based on the values of the diffusion coefficient of Li(I) and C_{Li} in the electrolyte. The diffusion-controlled current can be expressed as follows:

$$I_{lim} = \left| nFD_{Li^+} \frac{\varepsilon(C_{anode} - C_{cathode})}{l\tau} \right| \quad (3)$$

where n is the number of transferred electrons (n = 1), F is the Faraday constant, and $C_{cathode}$ and C_{anode} are the molar concentration of Li(I) at the surfaces of cathode and anode, respectively. To ensure the simplicity of this mathematical model, the convection and migration processes in the electrolyte are not taken into account in Eq. (3). Eq. (3) was used to estimate the limiting current on the assumption that: (i) the Li(I) concentration at the cathode ($C_{cathode}$) and anode electrode (C_{anode}) are 0 and 2 × C_{Li}, respectively, taking account of material balance in the cell, (ii) the Li(I) concentration changes linearly as a function of the electrolyte thickness, and (iii) the diffusion coefficient obtained by means of PGSE-NMR represents the mean diffusion coefficient for the whole electrolyte. Despite these simplifications, the predicted current density is more or less consistent with the experimental value, which is also shown in Fig. 5. However, the predicted value deviated from the experimental value at relatively low values of C_{Li}, probably because the concentration gradient of Li(I) is not uniform within the space between two Li electrodes. The viscosity of the liquid and the diffusivity of Li(I) change depending on the concentration of Li(I). The viscosity profile under the concentration gradient in the electrolyte will need to be further investigated for a more accurate prediction.

As demonstrated in this paper, the limiting current densities in ILs for lithium batteries are dominated by the diffusion process of Li(I). We estimated that the maximum limiting current density is 0.32 mA cm^{-2} for a single separator (21 μm-thick and porosity of 43%), as shown in Fig. 4(b). Unfortunately, this current density is not high enough for the practical application of ILs in high power lithium batteries. It should be noted that a battery cannot be charged and discharged at current densities higher than the limiting current density. Although the charge–discharge rate of a lithium ion battery is determined by many factors, the Li(I) transport properties of the electrolytes, particularly in the case of viscous electrolytes, have a significant effect on the charge–discharge rate capability of a battery. It is possible to increase the limiting current density in ILs by reducing the resistance of the separator layer; for example, the use of separators of a relatively high porosity and low tortuosity should be instrumental in achieving the desired limiting current density.

4. Conclusions

The self-diffusion coefficients of Li^+, $DEME^+$, and $TFSA^-$ in a LiTFSA/DEMETFSA binary IL were measured by PGSE-NMR. We found that the self-diffusion coefficient of each ionic species decreased with increasing concentration of LiTFSA. The limiting current density in the LiTFSA/DEMETFSA binary IL electrolyte was evaluated using a symmetric Li|IL|Li cell. The diffusion process of Li(I) in the IL dominates the limiting current density in the cell. The highest limiting current density is achieved at a concentration of 0.64 mol dm^{-3} of LiTFSA. In addition to the Li(I) transport properties of the electrolyte, the porosity, and tortuosity of the separator have significant effect on the limiting current density.

Acknowledgements

This study was supported in part by the Technology Research Grant Program from the New Energy and Industrial Technology Development Organization (NEDO) of Japan and the Nippon Sheet Glass Foundation for Materials Science and Engineering.

References

[1] H. Sakaebe, H. Matsumoto, Electrochem. Commun. 5 (2003) 594.
[2] B. Garcia, S. Lavallée, G. Perron, C. Michot, M. Armand, Electrochim. Acta 49 (2004) 4583.
[3] T. Sato, T. Maruo, S. Marukane, K. Takagi, J. Power Sources 138 (2004) 253.
[4] H. Sakaebe, H. Matsumoto, K. Tatsumi, J. Power Sources 146 (2005) 693.
[5] H. Matsumoto, H. Sakaebe, K. Tatsumi, M. Kikuta, E. Ishiko, M. Kono, J. Power Sources 160 (2006) 1308.
[6] M. Holzapfel, C. Jost, A. Prodi-Schwab, F. Krumeich, A. Würsig, H. Buqa, P. Novák, Carbon 43 (2005) 1488.
[7] S. Seki, Y. Kobayashi, H. Miyashiro, Y. Ohno, A. Usami, Y. Mita, N. Kihira, M. Watanabe, N. Terada, J. Phys. Chem. B 110 (2006) 10228.
[8] S. Seki, Y. Kobayashi, H. Miyashiro, Y. Ohno, A. Usami, Y. Mita, M. Watanabe, N. Terada, Chem. Commun. (2006) 544.
[9] A. Fernicola, F. Croce, B. Scrosati, T. Watanabe, H. Ohno, J. Power Sources 174 (2007) 342.
[10] S. Seki, Y. Ohno, Y. Kobayashi, H. Miyashiro, A. Usami, Y. Mita, H. Tokuda, M. Watanabe, K. Hayamizu, S. Tsuzuki, M. Hattori, N. Terada, J. Electrochem. Soc. 154 (2007) A173.
[11] H. Sakaebe, H. Matsumoto, K. Tatsumi, Electrochim. Acta 53 (2007) 1048.
[12] H. Nakagawa, Y. Fujino, S. Kozono, Y. Katayama, T. Nukuda, H. Sakaebe, H. Matsumoto, K. Tatsumi, J. Power Sources 174 (2007) 1021.
[13] S. Seki, Y. Kobayashi, H. Miyashiro, Y. Ohno, Y. Mita, A. Usami, N. Terada, M. Watanabe, Electrochem. Solid-State Lett. 8 (2005) A577.
[14] S. Seki, Y. Ohno, H. Miyashiro, Y. Kobayashi, A. Usami, Y. Mita, N. Terada, K. Hayamizu, S. Tsuzuki, M. Watanabe, J. Electrochem. Soc. 155 (2008) A421.
[15] S. Seki, Y. Kobayashi, H. Miyashiro, Y. Ohno, Y. Mita, N. Terada, P. Charest, A. Guerfi, K. Zaghib, J. Phys. Chem. C 112 (2008) 16708.
[16] V. Borgel, E. Markevich, D. Aurbach, G. Semrau, M. Schmidt, J. Power Sources 189 (2009) 331.
[17] Y. Wang, K. Zaghib, A. Guerfi, F.F.C. Bazito, R.M. Torresi, J.R. Dahn, Electrochim. Acta 52 (2007) 6346.
[18] R. Wibowo, S.E. Ward Jones, R.G. Compton, J. Phys. Chem. B 113 (2009) 12293.
[19] I. Nicotera, C. Oliviero, W.A. Henderson, G.B. Appetecchi, S. Passerini, J. Phys. Chem. B 109 (2005) 22814.
[20] O. Borodin, G.D. Smith, W. Henderson, J. Phys. Chem. B 110 (2006) 16879.
[21] Y. Saito, T. Umecky, J. Niwa, T. Sakai, S. Maeda, J. Phys. Chem. B 111 (2007) 11794.
[22] T. Frömling, M. Kunze, M. Schönhoff, J. Sundermeyer, B. Roling, J. Phys. Chem. B 112 (2008) 12985.
[23] K. Hayamizu, S. Tsuzuki, S. Seki, Y. Ohno, H. Miyashiro, Y. Kobayashi, J. Phys. Chem. B 112 (2008) 1189.
[24] H. Tokuda, K. Hayamizu, K. Ishii, M.A.B.H. Susan, M. Watanabe, J. Phys. Chem. B 108 (2004) 16593.
[25] H. Tokuda, K. Hayamizu, K. Ishii, M.A.B.H. Susan, M. Watanabe, J. Phys. Chem. B 109 (2005) 6103.
[26] H. Tokuda, K. Ishii, M.A.B.H. Susan, S. Tsuzuki, K. Hayamizu, M. Watanabe, J. Phys. Chem. B 110 (2006) 2833.
[27] A. Martinelli, A. Matic, P. Jacobsson, L. Börjesson, A. Fernicola, B. Scrosati, J. Phys. Chem. B 113 (2009) 11247.
[28] A. Webber, J. Electrochem. Soc. 138 (1991) 2586.
[29] K. Hayamizu, Y. Aihara, H. Nakagawa, T. Nukuda, W.S. Price, J. Phys. Chem. B 108 (2004) 19527.
[30] A. Shirai, K. Fujii, S. Seki, Y. Umebayashi, S. Ishiguro, Y. Ikeda, Anal. Sci. 24 (2008) 1291.
[31] I.V. Thorat, D.E. Stephenson, N.A. Zacharias, K. Zaghib, J.N. Harb, D.R. Wheeler, J. Power Sources 188 (2009) 592.
[32] M. Doyle, J. Newman, A.S. Gozdz, C.N. Schmutz, J.M. Tarascon, J. Electrochem. Soc. 143 (1996) 1890.